

Article

Influence of *Chrysoporthe deuterocubensis* Canker Disease on the Chemical Properties and Durability of *Eucalyptus urograndis* against Wood Rotting Fungi and Termite Infestation

Rasdianah Dahali ¹, Seng Hua Lee ^{2,*}, Paridah Md Tahir ^{1,3,*}, Sabiha Salim ³,
Muhammad Syahmi Hishamuddin ³, Atikah Che Ismail ³, Pui San Khoo ⁴, Tomasz Krystofiak ^{5,*}
and Petar Antov ⁶

- ¹ Institute of Tropical Forestry and Forest Products (INTROP), Universiti Putra Malaysia, Serdang 43400, Selangor, Malaysia
² Department of Wood Industry, Faculty of Applied Sciences, Universiti Teknologi MARA (UiTM) Cawangan Pahang Kampus Jengka, Bandar Tun Razak 26400, Pahang, Malaysia
³ Faculty of Forestry and Environment, Universiti Putra Malaysia, Serdang 43400, Selangor, Malaysia
⁴ Centre for Advanced Composite Materials (CACM), Faculty of Mechanical Engineering, Universiti Teknologi Malaysia, Johor Bahru 81310, Johor, Malaysia
⁵ Faculty of Forestry and Wood Technology, Poznan University of Life Sciences, 60-637 Poznan, Poland
⁶ Faculty of Forest Industry, University of Forestry, 1797 Sofia, Bulgaria
* Correspondence: leesenghua@hotmail.com (S.H.L.); parida.introp@gmail.com (P.M.T.); tomasz.krystofiak@up.poznan.pl (T.K.)



Citation: Dahali, R.; Lee, S.H.; Md Tahir, P.; Salim, S.; Hishamuddin, M.S.; Che Ismail, A.; Khoo, P.S.; Krystofiak, T.; Antov, P. Influence of *Chrysoporthe deuterocubensis* Canker Disease on the Chemical Properties and Durability of *Eucalyptus urograndis* against Wood Rotting Fungi and Termite Infestation. *Forests* **2023**, *14*, 350. <https://doi.org/10.3390/f14020350>

Academic Editor: Miha Humar

Received: 17 January 2023

Revised: 6 February 2023

Accepted: 6 February 2023

Published: 9 February 2023



Copyright: © 2023 by the authors. Licensee MDPI, Basel, Switzerland. This article is an open access article distributed under the terms and conditions of the Creative Commons Attribution (CC BY) license (<https://creativecommons.org/licenses/by/4.0/>).

Abstract: In this study, the effects of stem canker disease caused by *Chrysoporthe deuterocubensis* on the chemical properties and durability of a *Eucalyptus* hybrid (*E. urophylla* × *E. grandis*) were investigated. Eleven-year-old healthy and infected trees were collected. The samples were grouped into four different classes based on the infection severity: healthy (class 1), moderately infected (class 2), severely infected (class 3), and very severely infected (class 4). The changes in chemical properties were evaluated via chemical analysis and Fourier transform infrared spectroscopy (FTIR) analysis. A resistance test against fungal decay (*Pcynoporus sanguineus* and *Caniophora puteana*) and termite (*Coptotermes curvoignathus*) was also performed. The results showed that reductions in cellulose and hemicellulose content from 53.2% to 45.4% and 14.1% to 13.9%, respectively, were observed in the infected samples. Meanwhile, the percentages of lignin and extractives increased from 18.1% to 20.5% and 14.6% to 20.2%, respectively. The resistance against fungi and termites varied between severity classes. Generally, infected wood behaved better than healthy wood in terms of durability against fungi and termites. The durability classes for both tests were significantly improved, from resistant to highly resistant and poor to moderately resistant, respectively. These results suggest that *E. urograndis* that is infected by *C. deuterocubensis* might have a better potential use in lumber production with regard to its durability and processing cost compared to pulp and paper products.

Keywords: *Eucalyptus urograndis*; *Chrysoporthe deuterocubensis*; infection classes; chemical analysis; FTIR analysis; fungal decay; termite attack

1. Introduction

Eucalyptus spp. is commonly used in indigenous reforestation programs in Australia, Brazil, South Africa, and China to meet the demands of various forest-based industries, with the majority used for veneer in plywood, pulp and paper, or charcoal [1]. It is popular due to its rapid growth, with trees being harvested between the ages of 6 and 7 years. Numerous cloning programs have begun in these countries to improve the quality of this material, primarily through the development of hybrid species [2–5]. In particular, hybrid

trees of *Eucalyptus urophylla* × *E. grandis*, also known as *E. urograndis*, represent the most commonly used hybrid for producing pulp, paper, and cellulose for industrial use [6,7]. The crossing of these two Eucalyptus species permits fast growth, a characteristic of *E. grandis*, as well as improved physical properties of the wood, i.e., increased wood density from 460 to 650 kg/m³, which is a characteristic of *E. urophylla*. It is also thought that this hybrid is well adapted to various ecological conditions [8]. According to Luo et al. [1], the majority of Eucalyptus plantations in China produce logs that are excellent for solid wood applications, such as veneer production, due to characteristics such as low taper, good straightness, desirable wood density, rigidity, and wood surface texture [9,10]. Therefore, hybrid clones of *E. urophylla* × *E. grandis* possess ideal characteristics in terms of both growth and density, with numerous industries continuing to invest in research on the genetic development of this hybrid [11–13]. Recently, fluctuations in the price of pulp and paper have caused many of the major forestry companies to begin considering alternative uses for Eucalyptus wood [14]. Factors such as scarcity and high cost of native woods, as well as ecological pressure from overharvesting, have contributed to the rise in the utilization of Eucalyptus wood materials, particularly in the flooring and lumber industry [15]. Although the major properties of wood from *E. urograndis* have been reported in terms of pulp and paper, studies specifically concerning the potential use of these materials in lumber products are lacking. Meanwhile, the utilization of Eucalyptus species, particularly Eucalyptus hybrids, in Malaysia is still new [16–18] and requires much attention and care, especially concerning the susceptibility of this hybrid to biological deterioration. According to research from other countries [18], *Eucalyptus* spp. is susceptible and vulnerable to disease and infection [19,20]; for example, disease had a negative impact on Eucalyptus plantations in many African countries [21].

Nonetheless, despite their promising future, Eucalyptus trees are vulnerable to fungal disease infection, particularly stem canker (*Chrysosporthe deuterocubensis*). Stem canker is one of the most important pathogens that infected and killed Eucalyptus trees in several Malaysian plantation locations [22]. The cankers cause broken limbs and trunks, stunted and distorted growth, and, frequently, mortality. This disease is known to kill a large number of trees, particularly in young plantations, and as a result, it is a major impediment to the successful establishment of Eucalyptus plantations [23]. The infected trees are normally left to rot on site without any intervention. This, however, raises two concerns. The first is that if it is left untreated, it may infect other healthy trees nearby. The second concern is whether the infected tree can be used in another way to avoid total loss. In this regard, we conducted a number of studies to investigate the effects of stem canker disease (*Chrysosporthe deuterocubensis*) infection on the physical, mechanical, and machining properties of *E. urograndis* in the Sabah plantation [24,25]. The results revealed that the strength properties of the infected trees were reduced. However, the reduction was minor, as the most severely damaged trees lost 21.3% of their modulus of rupture when compared to healthy trees, while lightly damaged trees lost only 11.6%. These infected trees are said to be suitable for non-structural applications such as furniture, interior finishing, window frames, and doors [24]. Infected trees, on the other hand, were found to have acceptable machining characteristics, justifying their use in furniture production [25].

Another important criterion for the efficient utilization of wood is its natural durability, particularly when applied externally. Despite the fact that the infected trees are still able to be used as furniture or door frames, their durability against fungi and termites still remains unknown. In addition to related research, the chemical properties and durability of infected *E. urograndis* against wood-degrading organisms such as fungi and termites were investigated. The primary goal of this study was to assess the impact of *C. deuterocubensis* infection on the chemical properties and durability of *E. urograndis* against wood rotting fungi and termite infestation. The relationship between severity classes and the extent of fungi and termite damage was also investigated.

2. Materials and Methods

Trees of 11-year-old *Eucalyptus urophylla* × *E. grandis* hybrid clones originating from China were collected in this study. The plantation was planted and managed by the company Sabah Softwoods Berhad, Tawau, Malaysia, with geographical coordinates 4°33'16.3" N, 117°42'58.7" E. The trees were planted in an entirely randomized block design with three types of planting spaces (1.5 m × 3 m, 1.8 m × 3 m, and 3 m × 3 m). The region where the experiment was deployed is about 11.7 ha and has a moist tropical climate with two well-defined seasons (dry and wet) [26]. The dry season lasts from May to September and the rainy season lasts from October to April. The infected trees were identified, and a forest pathologist confirmed by visual examination that the pathogen that attacked the trees was *C. deuterocubensis* [20]. Pictures were taken, the characteristics of the infection were recorded, and the extent of the infection was determined based on the severity of the symptoms that occurred. Based on careful examinations of the pictures, as well as the physical symptoms/characteristics of the disease and its percentage of occurrence, the infected trees were grouped into four classes according to the severity of the infection, as depicted in Table 1. Meanwhile, Table 2 displays the physical properties of healthy and infected *E. urograndis* wood that have been observed from our previous study [24] such as equilibrium moisture content (EMC), density, and volumetric shrinkage (Vol_{sh}).

Table 1. Classes of severity for *Eucalyptus urograndis* infected with *Chrysosporthe deuterocubensis* ^a.

Class	Category	Symptom
1	Healthy	Stem appears normal without any symptom of being infected
2	Moderate	Swollen bark (callus) Cracking Fruiting structure Fresh kino pocket Canker
3	Severe	Swollen bark (callus) Cracking Fruiting structure Fresh kino pocket and fresh kino/gummosis Canker Sunken Rotten
4	Very severe	Swollen bark (callus) Cracking Fruiting structure Dried kino pocket & dried kino/gummosis Canker Sunken Rotten Shoot

^a Adapted with permission from Rasdianah et al. [24].

Table 2. Physical properties of *Eucalyptus urograndis* ^a.

Infection Classes	EMC (%)	Density (Kg/m ³)	Vol _{sh} (%)
1	10.5	670.8	15.1
2	10.1	618.9	14
3	10.2	706.8	14.5
4	9.7	542.3	12.9

^a Adapted with permission from Rasdianah et al. [24].

2.1. Evaluation of Chemical Properties

2.1.1. Wet Chemical Analysis

Small splints (1 to 2 cm long) were taken from each infection class after conditioning for evaluation of their chemical properties. To produce sawdust, the splints were ground using a Wiley cutting mill (Wiley, Model 4, Swedesboro, NJ, USA); to obtain homogeneous sizes, sawdust was screened using a 40 to 60 mesh (0.4 to 0.6 mm) sieve according to the Technical Association of the Pulp and Paper Industry (TAPPI) standard method, T 257 cm-02 [27]. The chemical composition analysis of *E. urograndis* particles was conducted at the Malaysian Agricultural Research and Development Institute (MARDI) lab, Serdang, by using neutral detergent fiber (NDF) and acid detergent fiber (ADF). This is a common way to evaluate the main fiber constituents, cellulose, hemicelluloses, and lignin. All chemical constituent percentages for each class of severity samples were determined as mean values of triplicate experiments.

2.1.2. Fourier Transform Infrared (FTIR) Analysis

The FTIR analysis was performed at the Biocomposite Laboratory of the Institute of Tropical Forestry and Forest Product (INTROP), UPM, using FTIR-attenuated total reflection (ATR) spectrometer instrument (iS10 FTIR, Thermo Nicolet, Durham, NH, USA) with spectrometer resolution of 0.4 cm^{-1} . The FTIR analysis was performed to qualitatively determine organic components, including chemical bond, functional group, and organic content (e.g., protein, carbohydrate, and lipid), and to correlate the result of chemical composition change from wet chemical analysis between different infection severity classes of the samples. The study included healthy samples as well as moderately, severely, and very severely (class 1, 2, 3, and 4) infected samples. As a control for comparison, a healthy sample was prepared. FTIR-ATR with a spectral range cutoff of 525 cm^{-1} was used to analyze the components of all samples. The particles were measured in the absorption mode using a mid-IR spectrum with wavenumbers ranging from $400\text{ to }4000\text{ cm}^{-1}$, and all spectra were plotted on the transmittance axis using the same scale [28].

2.2. Evaluation of Biological Properties

2.2.1. Decay Resistance

The decay resistance test was determined by exposing the samples ($20\text{ mm} \times 20\text{ mm} \times 10\text{ mm}$) to white rot and brown rot fungi (namely *Pycnoporus sanguineus* (WML 006) and *Coniophora puteana* (WML 004)) in a soil block test for 12 weeks according to procedures outlined in ASTM D2017 standard [29]. These fungi (Figure 1a,b) were collected from the Mycology and Pathology Laboratory, Forest Research Institute Malaysia (FRIM) cultured collection. These fungi were chosen because they are widely distributed in tropical regions. Even in allegedly durable timber, they cause significant damage [30]. Twenty replicates of each class of severity (class 1, 2, 3, and 4) were tested against each fungus. The test blocks were labeled and oven-dried at $103 \pm 2\text{ }^\circ\text{C}$ until they reached a constant weight. The blocks initial weight was then recorded as W_1 . Each culture bottle contained 150 g of sieved soil and 70 mL of distilled water. Feeder strips of pine wood ($35\text{ mm long} \times 28\text{ mm wide} \times 3\text{ mm thick}$) were placed on top of the soil in each culture bottle for fungal inoculation. The bottles with the feeder strips were loosely capped and steam-sterilized at $121\text{ }^\circ\text{C}$ for 20 min before being cooled in laminar flow under ultraviolet light at room temperature.

The fungus was placed at the corner of the feeder strip after cooling. Then, the bottles were incubated at a temperature of $27 \pm 2\text{ }^\circ\text{C}$ and 70% relative humidity for approximately 3 weeks until the mycelium fully covered the feeder strips. Then, the test blocks were placed on top of the feeder strips and incubated for 12 weeks of fungal exposure. The test blocks were taken out from the bottles at the end of the incubation period, and all mycelium on the test block surfaces was removed. The degree of fungal attack was estimated by determining the weight loss of the test block. The test blocks were then oven-dried until

they reached a constant weight, W_2 . After weighing each block, the percentage of weight loss (WL_{decay}) for the test block was calculated using Equation (1):

$$WL_{\text{decay}} (\%) = 100 (W_1 - W_2) / W_1 \quad (1)$$

where W_1 is the initial weight of the test block before exposure to fungus (g) and W_2 is the final weight of the test block after exposure to fungus (g).

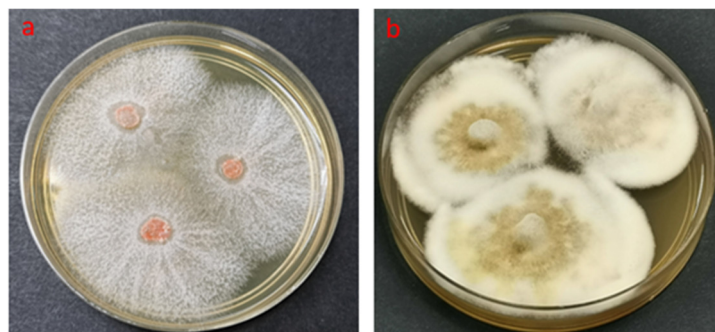


Figure 1. White rot (a) (*Pycnoporus sanguineus*) and brown rot (b) (*Coniophora puteana*) fungi isolates grown on malt extract agar (MEA) media.

Table 3 lists the assignment of resistance classes based on the mean weight loss of the samples caused by fungal decay.

Table 3. Classification of decay resistance according to weight loss values ^c.

Sample Condition	Mean Weight Loss (%)	Resistance Class
Highly resistant	0–10	I
Resistant	11–24	II
Moderately resistant	25–44	III
Slightly resistance or non-resistant	≥45	IV

^c Adapted from ASTM standard D2017 [29].

2.2.2. Termite Resistance

A no-choice termite resistance test with *Coptotermes curvignathus* Holmgren (subterranean termites) was performed according to the American Wood Protection Association (AWPA) standard E1-09 procedure [31]. The termites were collected from an infested pine plantation at Institute of Biosciences, Universiti Putra Malaysia. The termite species was confirmed both morphologically and genetically with references from previous study [32]. *C. curvignathus*, as shown in Figure 2, is one of the most common species of termite [33], and causes severe damage to forest trees, wooden structures, and buildings [30,34,35]. They are also the only species of termite capable of establishing secondary nests that allow them to attack high-level buildings [36]. Living trees can also be attacked by this species in their inner and outermost parts. A total of 20 replicates (20 mm × 20 mm × 7mm) for each sample of severity class were tested. A sample was placed in a glass container containing 200 g of sterilized sand and 30 mL of distilled water with 1 ± 0.05 g of *C. curvignathus*. *C. curvignathus*, consisting of 90% workers and 10% soldiers, were weighed and placed in each bottle.

In this study, only vigor and active termites were used. A sample from each severity class was randomly selected and conditioned at 20 °C until it reached a constant weight. The initial weight of the blocks, W_i , was measured before they were placed in sterilized test bottles filled with sand. The cultured bottles were incubated and maintained at a temperature of 27 ± 2 °C and 70% relative humidity for approximately 4 weeks. After 4 weeks, the test block samples were taken out of the cultured bottles and brushed off to eliminate sand particles. All samples were oven-dried until a constant weight, W_f , was

achieved. The efficacy of severity class infection was evaluated based on the percentage weight loss of the materials due to termite attack. Using Equation (2), each test block was examined based on the percentage of weight loss (WL_{termites}). Classification of the durability classes was carried out according to the Indonesian National Standard SNI 01.7207 [37], based on the weight loss criteria developed (Table 4). Each sample was also rated based on the visual evaluation system provided by the AWPA standard E1-09 [31] in Table 5.



Figure 2. Subterranean termites (*Coptotermes curvignathus*) collected from infested pine plantation at Institute of Bio-science, UPM.

$$WL_{\text{termites}} (\%) = 100 (W_i - W_f) / W_i \quad (2)$$

where W_i is the initial weight of the test block before exposure to termites (g) and W_f is the weight of the test block after exposure to termites (g).

Table 4. Classification of termite resistance according to weight loss values ^d.

Sample Condition	Mean Weight Loss (%)	Resistance Class
Very resistant	<3.52	I
Resistant	3.52–7.50	II
Moderate	>7.50–10.96	III
Poor	>10.96–18.94	IV
Very poor	>18.94	V

^d Adapted from standard SNI 01.7207 [37] and Terzi et al. [38].

Table 5. Rating system for visual evaluations of termite resistance ^e.

Visual Rating Classification	Rating
Sound	10
Trace, surface nibbles permitted	9.5
Slight attack, up to 3% of cross-sectional area affected	9
Moderate attack, 3%–10% of cross-sectional area affected	8
Moderate/severe attack, penetration, 10%–30% of cross-sectional area affected	7
Severe attack, 30%–50% of cross-sectional area affected	6
Very severe attack, 50%–75% of cross-sectional area affected	4
Failure	0

^e Adapted from AWPA standard E1-09 [31].

2.3. Statistical Analysis

To determine how the different infection classes affected the chemical changes and durability of the *E. urograndis* wood, a one-way analysis of variance (ANOVA) was used to analyze and interpret the data. The discrepancies between the mean values of each severity class were investigated further using Duncan's multiple range (DMR) test at $p \leq 0.05$. Pearson's correlation coefficients were used to assess the relationships between infection classes and weight loss due to fungal decay (WL_{decay}) and termite attack (WL_{termites}). All statistical analyses were performed using SPSS version 22.0. (IBM, Armonk, NY, USA).

3. Results and Discussion

3.1. Chemical Properties of Healthy and Infected Wood

Table 6 shows the chemical composition of 11-year-old healthy and infected *E. urograndis* wood. *E. urograndis* has a cellulose content of more than 45% on average. A maximum cellulose content of 53.2% was determined in the healthy (class 1) *E. urograndis* compared to the infected (class 2, 3 and 4) trees, which had cellulose contents of 50.9%, 49.8%, and 45.4%, respectively. A downward trend was observed as the cellulose content decreased, as the extent of the trees' infections were becoming severer. Similar to cellulose, hemicellulose content was also reduced as the severity of the infection increased. Meanwhile, lignin and extractive content increased. However, the changes were interdependent, as a decrease in hemicellulose content was accompanied by an increase in lignin, and vice versa.

Table 6. Mean values of chemical composition of *Eucalyptus urograndis* wood.

Severity Classes	Chemical Composition (%)			
	Cellulose	Hemicellulose	Lignin	Other Component
1 (Healthy)	53.2	14.1	18.1	14.6
2 (Moderate)	50.9	11.2	19.9	18.0
3 (Severe)	49.8	11.6	19.0	19.6
4 (Very severe)	45.4	13.9	20.5	20.2

Aromatic rings with multiple potential branches characterize amorphous lignin. It acts as a binding agent for individual cells, as well as for the fibrils that make up the cell wall. Lignin first forms between adjacent cells in the middle lamella, tightly bonding them to form a tissue. It then spreads through the cell wall, penetrating hemicellulose and bonding cellulose fibrils. Lignin provides compressive strength and stiffness to the cell wall of tree tissue and individual fibers, protecting the carbohydrate from physical and chemical damage. The amount of lignin effects the structure, properties, morphology, and flexibility of wood [39]. According to Ferrari et al. [40] and Savory and Pinion [41], the ascomycete fungi are able to break down lignin, albeit inefficiently. Contrary to that, Andlar et al. [42], Janusz et al. [43], and Kirk and Farrell [44] stated that ascomycete fungi are unable to degrade lignin and only consume the easy to-access hemicellulose and cellulose. In this study, it can be seen in Table 6 that the lignin content of infected *E. urograndis* is higher (19.9%, 19.0%, and 20.5%) than in the healthy (18.1%) sample. This fact is in agreement with previous studies by Mafia et al. [45] and Foelkel et al. [46]. The authors observed the increase in the proportions of lignin and extractives when they analyzed the wood from *Eucalyptus* trees with canker caused by *Cryphonectria cubensis* (Bruner) Hodges.

Wood extractives are natural products that exist independently of a lignocellulose cell wall. They are present within the cell wall, but are not chemically connected to it. Aromatic phenolic compounds, aliphatic compounds (fats and waxes), terpenes, and terpenoids, as well as a variety of other minor organic compounds, are among these compounds [47,48]. In their study, Shebani et al. [49] discovered that *Eucalyptus* spp. wood contains more polar extractives, which include tannins, gums, sugars, starches, and colored matter. The phenolic compounds affect fungal physiology directly. As previously stated, aliphatic compounds

can act as surfactants, limiting fungal adhesion to wood surfaces. The phenolic compounds are classified into four groups: lignans, stilbenes, flavonoids, and tannins [50,51]. These extractives are molecules produced by trees to protect themselves from biotic and abiotic stressors. The proportion of other components in infected samples classes 2, 3, and 4 was higher than in healthy samples (class 1). As the infection progressed, the extractive content increased steadily from 18.6% to 20.2%, compared to 14.6% in the healthy samples. A similar result was found in a study on a *Eucalyptus grandis* hybrid by Mafia et al. [45]. According to the author, after being infected with *Ceratocystis fimbriata* wilt, the proportion of extractives and lignin increased.

Based on this result, it can be said that *C. deuterocubensis* causes a chemical change to *E. urograndis* wood, as the infected wood contained less cellulose and hemicellulose than the healthy wood. This fungus enters the tree via injuries to the bark. It then spreads to the underlying vascular cambium, destroying these tissues as it advances, degrading some or all major cell wall components, and absorbing breakdown products of cellulose or hemicellulose. This finding was supported by the previous study conducted by Dahali et al. [24] on the physical properties of *E. urograndis*, where it was found that the fiber saturation point, equilibrium moisture content, density, and volumetric shrinkage of infected wood were lesser than in healthy trees. A work conducted by Gunduz et al. [52], Fernandez et al. [53], and Mafia et al. [54] also obtained similar results. These authors reported that the holocellulose content of infected wood decreased compared to that of the healthy trees. It is presumed that the decrease in cellulose and hemicellulose in cell material was caused by a fungal disease utilizing cellulose and hemicellulose as energy and carbon sources for its colonization progresses.

In contrast, infected samples contained higher levels of extractives and lignin [53]. Other studies, including Foelkel et al. [46] and Souza et al. [55], have demonstrated the influence of the *Chrysosporthe cubensis* disease on the quality of Kraft pulp. It was found that the infected wood of *E. grandis* and *E. saligna* presented higher levels of extractives and lignin content compared with healthy wood, causing a 1% loss in the pulp yield and a 10% loss in volume. The increase in these components could be due to the activation of the tree's defense mechanisms, which also results in the production of chemicals, gums, and tyloses [56]. In response to infection, the plant may trigger reactions that prevent fungus penetration or limit fungus colonization in host tissues, such as extractive, lignin, and other phenolic compound accumulation [57,58]. According to Kuc [59], lignification in plants can increase the pathogen's inability to penetrate the cell walls. Trees' defense mechanisms can prevent the invasion of pathogens or wood-rotting fungi, and response zones containing lignin act as barriers to their invasion and colonization [60]. The reaction zones, however, are not always effective against microbial penetration. Changes in the cell wall and occlusion of xylem elements are examples of activated defense mechanisms. These plant responses may limit pathogen development in wood [61]. Histochemical and biochemical studies revealed that phenolic compounds associated with phytoalexin production accumulated in *Platanus acerifolia* plants inoculated with *Ceratocystis platani* [62].

3.2. Fourier-Transform Infrared Spectroscopy (FTIR) Analysis

The FTIR was run to qualitatively determine the alteration of chemical properties and functional groups present in healthy and infected *E. urograndis*. Figure 3 illustrates the FTIR spectra that display the common components or functional groups, such as cellulose, hemicellulose, and lignin, at a wavenumber ranging from 4000 to 525 cm^{-1} .

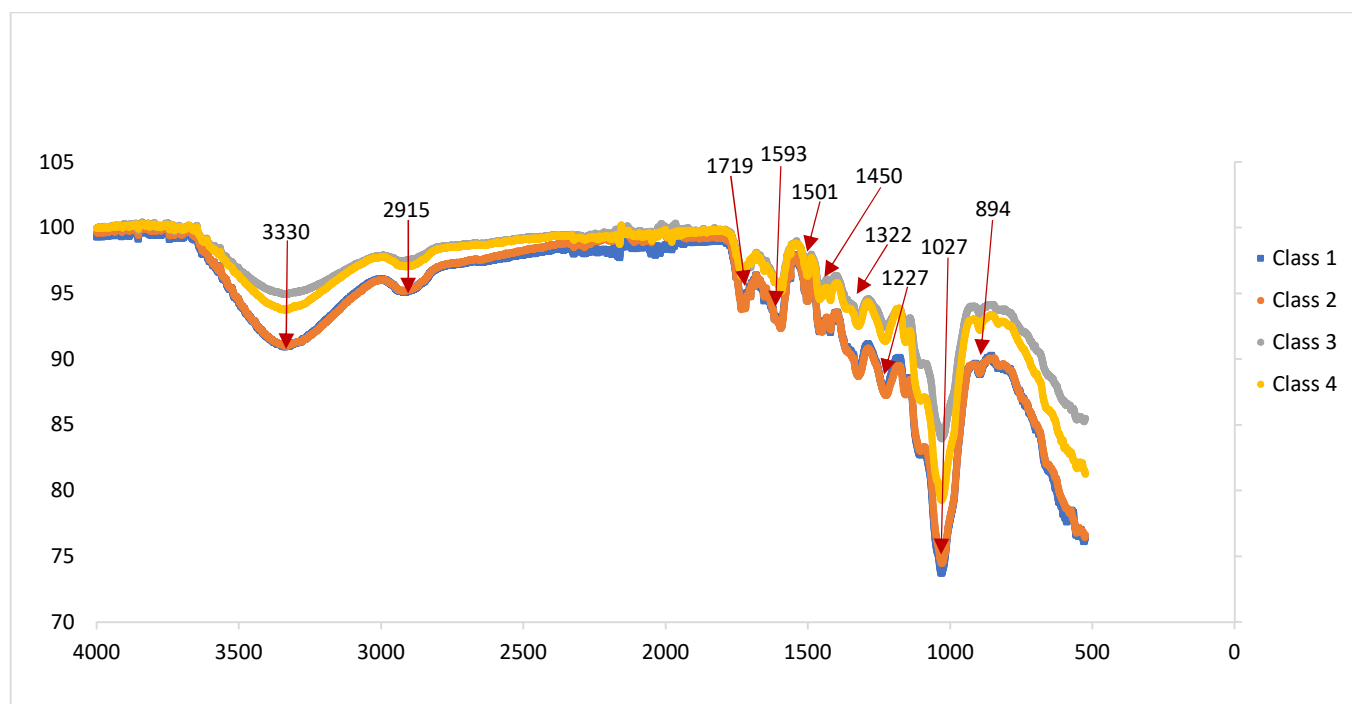


Figure 3. FTIR spectra (4000 cm^{-1} – 525 cm^{-1}) of healthy (class 1) and infected samples *Eucalyptus urograndis* (class 2, 3 and 4).

Table 7 depicts the important bands that can be found in an infrared spectrum of wood and includes their functional assignment. The result demonstrated that numerous peaks were detected, and that it is difficult to interpret the differences between the spectra of healthy and infected wood since there are several reactions occurring at the same time. The first single bond region showed that a broadening absorption of the band (3570 – 3200 cm^{-1}) is assigned to stretching vibrations of intra-molecular hydrogen bonds in the crystalline regions of cellulose, which shift from 3340 – 3330 cm^{-1} in the spectrum [63]. This band also confirms the existence of hydrate (H_2O), hydroxyl group ($-\text{OH}$), ammonium, or amino. This broadening might be due to the reduction in O-H stretch, which represents decrement of polysaccharides as a result of infection by *C. deuterocubensis*. Like humans, this fungus needs carbohydrates (celluloses and hemicelluloses) for carbon skeletons and energy sources. They also require amino acids to combine with carbon skeletons to synthesize proteins for their growth and enzymes. As a result, infected classes 2, 3, and 4 lost density and moisture content because the components of the cell walls were degraded, resulting in fewer free OH- groups and fewer water molecules binding to the cells. This indicated that the samples had lower hydrophilic properties [24,64]. Simultaneously, O-H from phenolic groups in lignin increases, as it is well known that the lignin percentage of the ratio increases due to carbohydrate degradation [65].

Table 7. Functional group in FT-IR spectra of the studied sample. Data were adopted from references [28,64,66,67].

Wavenumber (cm^{-1})	Functional Group/Band Assignment
3570–3200 (broad)	-OH stretching hydrogen bonds in cellulose
2935–2915	Asymmetric -CH stretching of methylene (CH_2) in lignin
1750–1700	C=O stretching of non-conjugated carbonyl compound in xylan
1615–1580	C=O aromatic ring stretching

Table 7. Cont.

Wavenumber (cm ⁻¹)	Functional Group/Band Assignment
1515–1500	Aromatic ring (benzene) stretching vibrations
1460	C-H deformations in xylan
1420	Aromatic ring of lignin and C-H bending in cellulose
1324–1322	CN stretching in ether and oxy compound, and stretching P=O in simple hetero-oxy compound
1225–950 (several)	Aromatic C-H in-plane bend
1190–1130	Secondary amine, CN stretch
1047–1004	C-O stretching in cellulose I and cellulose II
896	Asymmetric C-H out-of-plane bending deformation in cellulose and hemicellulose

The band at 2920 to 2915 cm⁻¹ corresponds to asymmetric -CH stretching vibration in the aromatic methyl and methylene groups of side chains generally found around 2935–2915 cm⁻¹. According to Moharram and Mahmoud [68] and Spiridon et al. [69], the apparent shift in frequency of the -CH band is due to structural and relative composition changes, specifically changes in the crystallinity level of the cellulose. The double bond region (1750 and 1700 cm⁻¹) represents the C=O stretching of non-conjugated carbonyl compounds that occurs in xylan, such as carboxylic acid (1725–1700 cm⁻¹), ketones (1725–1705 cm⁻¹), aldehydes (1740–1725 cm⁻¹), esters (1750–1725 cm⁻¹), and 6 membered rings of lactone (1735 cm⁻¹) [28]. In comparison to healthy wood, the intensities of these bands increased as the infection class became more severe. The increase in lignin content that derived from the carbohydrate loss could be observed as the increase in these bands, which is due to the formation of carbonyl groups in lignin [70].

According to Nandiyanto et al. [28] and Esteves et al. [67], the absorption peak which occurred around 1615–1580 cm⁻¹ was due to vibrations in the aromatic ring of lignin and C=O stretching. The band at 1593 cm⁻¹ shifted to about 1596 cm⁻¹ for healthy and infected wood, respectively. This band increases due to an increase in the percentage of lignin in the infected wood [71]. The band at the fingerprint region of 1460 cm⁻¹ corresponds to the asymmetric deformation of the C-H bond of xylan, while the band at 1420 cm⁻¹ corresponds to the vibration of the lignin's aromatic ring, but also to the C-H bending in the cellulose [72].

Aromatic rings exhibit, most of the time, a characteristic band at approximately 1224 to 1228 cm⁻¹. The presence of an absorption in the range of 1156–1158 cm⁻¹ was noted in the FTIR spectra, and this belongs to the stretching vibrations of the symmetric cellulose C-O-C (1155–1159 cm⁻¹), which corresponds to the content in crystallized and amorphous cellulose. In their study, Gelbrich et al. [73] reported that the band at 1031 cm⁻¹ (class 1) was assigned to bonds of holocellulose (1047–1004 cm⁻¹) and that the intensity of the band decreased as the infection became more severe, indicating the lessened polysaccharide content. The attack of a fungal disease infection on polysaccharides (sugar ring tension) is clear by the decreased band intensities at 896–893 cm⁻¹, corresponding to the pyranose ring opening. Similar results were obtained by Kotilainen et al. [71] and Pena et al. [74]. Meanwhile, the fungi's enzymatic activity is primarily responsible for the decrease in intensities of asymmetric and C-H out-of-plane stretching of cellulose and hemicellulose.

3.3. Durability

3.3.1. Fungal Decay

Figure 4 shows that mycelium covered the surfaces of the test blocks, particularly the healthy one (class 1). It can be observed that the healthy samples were heavily colonized by fungi when compared to the infected test blocks (class 2, 3, and 4).

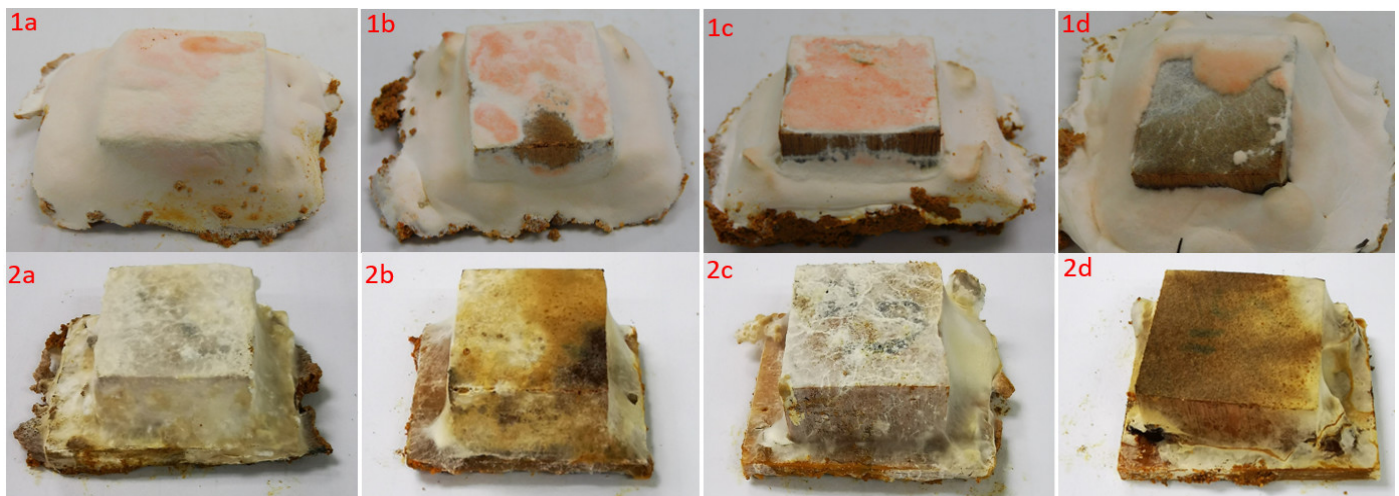


Figure 4. Visual appearance of healthy and infected *E. urograndis* against *P. sanguineus* (upper): **1a** = class 1, **1b** = class 2, **1c** = class 3, and **1d** = class 4; and *C. puteana* (lower): **2a** = class 1, **2b** = class 2, **2c** = class 3, **2d** = class 4.

Table 8 shows the durability *E. urograndis* of classes 1, 2, 3, and 4 after being exposed to *P. sanguineus* and *C. puteana* for about 12 weeks. As presented in Table 8, the results revealed that the WL_{decay} decreased progressively. *P. sanguineus* caused more WL_{decay} than *C. puteana*, with values ranging from 14.4% to 9.5% and 11.2% to 6.1% for healthy and infected samples, respectively. It was observed that the WL_{decay} of the infected samples caused by both *P. sanguineus* and *C. puteana* was significantly lower than that of the healthy samples. It was noted that the white rot fungi caused severer damage on the *Eucalyptus* trees compared to brown rot fungi. The results show that a significant improvement was recorded for the resistance of infected samples against both *P. sanguineus* and *C. puteana*, as indicated by the lower WL_{decay} found in the infected samples (class 2, 3, and 4). Thus, the durability classes of infected samples were also improved, from resistant (class 1) to highly resistant (class 4), against *P. sanguineus* and *C. puteana*.

Table 8. Mean weight loss and durability classes of infected and healthy *Eucalyptus urograndis* against white rot and brown rot fungal decay.

Infection Classes	Value	WL_{decay} (%)		Resistance Classes	
		<i>P. sanguineus</i>	<i>C. puteana</i>	<i>P. sanguineus</i>	<i>C. puteana</i>
1 (Healthy)	Mean	14.4 ^a	11.2 ^a	Resistant (II)	Resistant (II)
	SD	2.7	2.8		
2 (Moderate)	Mean	12.3 ^b	8.0 ^b	Resistant (II)	Highly resistant (I)
	SD	3.0	2.3		
3 (Severe)	Mean	10.3 ^c	7.8 ^c	Highly resistant (I)	Highly resistant (I)
	SD	2.5	3.1		
4 (Very severe)	Mean	9.5 ^c	6.1 ^c	Highly resistant (I)	Highly resistant (I)
	SD	1.9	2.6		
<i>p</i> -value		0.000 ***	0.000 ***		

Notes: Classification of decay resistance according to ASTM standard D2017 [29]. Means followed by the same letter (a, b, c) in the same column were not significantly different at $p < 0.05$ according to Duncan's multiple range test. ***, high significance ($p < 0.01$); ***, very high significance ($p < 0.001$).

This observation was made due to the increase in lignin and extractive content of *E. urograndis* after *C. deuterocubensis* tree infection, which helped to deter the wood from decay. Samples of classes 3 and 4 showed high resistance against white rot fungi, while classes 2, 3 and 4 showed high resistance against brown rot fungi. Owing to the lower

availability of polysaccharides to consume by the *P. sanguineus* and *C. puteana*, the increase in lignin instead of cellulose and hemicellulose is not favorable for the growth of *C. puteana* (brown rot) fungi. Brown rot fungi mainly degrade cellulose and hemicelluloses and leave most of the lignin undegraded [75,76]. Another plausible reason for the decrement of WL_{decay} was the lower density and equilibrium moisture content (EMC) of infected than healthy wood. In our previous study [24] we found that infected samples of classes 2, 3, and 4 had low density (618.9, 706.8, and 542.3 kg/m³) and moisture content (10.1, 10.2, and 9.7%) values, respectively. This phenomenon is thought to be stressful for fungal growth. Moisture is required for all processes in wood infected by decay fungi, including spore arrival and germination, mycelial growth, and wood metabolism. As a result of the lower hydrophilic properties of infected wood (decrease in MC of wood), the growth and colonization of wood-decaying fungi were minimized, making decaying fungi less able to grow and degrade wood [77].

A study by Gunduz et al. [52] on chestnut wood infected by *Cryphonectria parasitica* (Murrill) found that vessel diameters and vessel frequency in the transverse section became smaller, and the lengths of the vessel elements were shorter. The formation of granular layers was observed via scanning electron microscopy (SEM) in the inner walls of the vessels. Moreover, Mafia et al. [55] found there was deposition of residual stromatic hyphae tissue in vessel of *E. urograndis*, caused by intense growth of *Hypoxylon* spp. It is likely that these structures resulted from the colonization activities of the *Hypoxylon* spp. disease. Thus, in this study, the penetration of both types of fungal decay (*P. sanguineus* and *C. puteana*) into wood vessels for colony growth may be limited due to vessel obstruction from a previous infection by *C. deuterocubensis*. A similar finding of the study by Clerivet and El Modafar [78] reported alteration in xylem vessels, including thickening of vessel walls, occlusion of pores, deposition of gels, gum, and formation of tyloses after inoculation of *Platanus acerifolia* with *Ceratocystis fimbriata* f. sp. platani. A study by Mafia et al. [45], by using SEM, found the presence of the pathogen structures and tyloses in *E. grandis* hybrid infected by *Ceratocystis fimbriata*. Tyloses are considered an active defense mechanism which involves partial or complete occlusion of xylem vessels through the deposition of gels and gummosis (kino) to limit microbial growth [79,80]. According to MTIB [81], the vessel of *Eucalyptus* spp. contained a moderate amount of tyloses and gums. *Eucalyptus* spp. is known as the “gum tree”, as it presents a gum canal (kino veins) and secretes a gooey substance. Timor white gum is known to come from *E. urophylla* [82], while flooded gum is known to come from *E. grandis* [83]. When the trunk surface of a gum tree is damaged, it oozes visible amounts of thick, gummy (resinous liquid) sap.

3.3.2. Termite Attack

The mean weight loss (WL_{termites}), increment of resistance, block visual rating, and class of resistance of healthy (class 1) and infected wood samples (class 2, 3, and 4) after 4 weeks of exposure to *C. curvignathus* are presented in Table 9. The results show that the WL_{termites} values decreased consistently from healthy to infected (class 4) samples.

From the experimental results, all sample blocks tested were attacked by termites, as reflected in Figure 5. The healthy sample (class 1), which had the highest WL_{termites} value of 20.1%, was attacked the most, followed by the infected samples in classes 2 (16.4%), 3 (12.5%), and 4 (9.9%). Significant resistance improvement was observed for the infected class 2 to class 4 samples, from very poor (V) to moderately resistant (III).

Based on the visual rating classification of termite attacks, the samples from classes 1, 2, 3, and 4 had rating values of 7, 7, 7, and 8, respectively. The results demonstrated a slight improvement for infected *E. urograndis*. This shows that as the lignin and extractive proportion and concentration increased, so did the resistance to the *C. curvignathus* attack [46]. The toxicity of lignin and extractives may have increased resistance and provided protection to infected *E. urograndis* against *C. curvignathus* termite feeding in our study. Another possibility is that the tree’s defense mechanisms were activated while or after the *E. urograndis* tree was infected with *C. deuterocubensis*, resulting in the formation of chemical

substances, such as gums, tyloses, and other phenolic compounds [57], which act as slow poisons to termites.

Table 9. Mean weight loss and durability classes of infected and healthy *Eucalyptus urograndis* against termite attacks.

Infection Classes	Value	WL _{termite} (%)	Visual Rating	Resistant Classes
1 (Healthy)	Mean SD	20.12 ^a 4.5	7	Very poor (V)
2 (Moderate)	Mean SD	16.44 ^{ab} 8.8	7	Poor (IV)
3 (Severe)	Mean SD	12.49 ^{bc} 5.5	7	Poor (IV)
4 (Very severe)	Mean SD	9.86 ^c 6.0	8	Moderately resistant (III)
<i>p</i> -value		0.000 ^{***}		

Notes: Classification of termite resistant according to SNI 01.7207 [37] and rating system according to AWPA standard E1-09 [31]. Means followed by the same letter (a, b, c) in the same column are not significantly different at $p < 0.05$ according to Duncan's multiple range test. **, high significance ($p < 0.01$); ***, very high significance ($p < 0.001$).



Figure 5. Condition of samples after exposure to termite attack; (a) = class 1, (b) = class 2, (c) = class 3, and (d) = class 4.

In addition, Bayle [84] and FAO [85] stated that more than 300 species of *Eucalyptus* are interspecific hybrid containing volatile oils, which consist of mixtures of hydrocarbons (terpenes and sesquiterpenes) and oxygenated compounds (alcohols, esters, ethers, aldehydes, ketones, lactones, phenols, and phenol ethers) [85–87]. These volatile oils have favorable properties that have insecticidal and antimicrobial properties [84,85]. Furthermore, vessel obstruction caused by *C. deuterocubensis* fungus infection may be another factor that deters termite attack.

3.4. Correlation between Infection Class and Weight Loss against Fungal Decay and Termite Attacks

Pearson's correlation between the infection class and WL_{decay} against *P. sanguineus* and *C. puteana*, as well as that between the infection class, WL_{termite}, and *C. curvignathus* in *E. urograndis* wood was conducted and tabulated in Table 10. The correlation was moderate, but highly significant ($p = 0.000$), in all durability tests. Generally, the weight loss from both fungal and termite tests decreased in trees of higher infection classes, as indicated by the weak negative correlations of WL_{decay}, *P. sanguineus* ($r = -0.594$), and *C. puteana* ($r = -0.540$), and of WL_{termite} and *C. curvignathus* ($r = -0.528$).

Table 10. Correlation between infection classes with weight loss against fungal decay and termite attack.

		Correlations			
		Class	Decay		Termite
			<i>P. sanguineus</i>	<i>C. puteana</i>	<i>C. curvignathus</i>
Class	Pearson correlation	1	−0.594 **	−0.540 **	−0.528 **
	Sig. (2-tailed)		0.000	0.000	0.000
	N	80	80	80	80

** Correlation is significant at the 0.01 level (2-tailed). ** Correlation is significant at the 0.05 level (2-tailed).

4. Conclusions

The chemical properties and biological durability of the *E. urograndis* trees infected by canker disease (*C. deuterocubensis*) were investigated in this study. The findings revealed that the cellulose and hemicellulose content decreased with increasing infection severity. On the contrary, lignin and extractive content increased as the severity of the infection increased. Consequently, the resistance of the infected tree against white rot and brown rot fungi was enhanced, probably due to the lower availability of polysaccharides in the infected wood on which the fungi could thrive. The resistance of the *E. urograndis* wood against subterranean termites was also improved. The resistance against termites improved from very poor in healthy samples (class 1) to moderately resistant in the most severely infected samples (class 4). Overall, the results showed that the infected wood had a high extractive content, which made it unsuitable for pulp and paper production. However, it may have some potential in lumber production, as it has more added value and a lower cost of production than pulp and paper products.

The current study expands on previous research into the physical, mechanical, and machining properties of infected *E. urograndis* wood. When compared to healthy trees, infected trees showed only a minor reduction in strength. Because of the minor strength reduction, they are appropriate for non-structural applications such as furniture, interior finishing, window frames, and doors. Furthermore, the infected wood has acceptable machining properties, justifying its use in furniture production. When combined with the current study's findings that the infected wood demonstrated improved biological durability, the case for using infected wood in non-structural applications is strengthened. This may assist the planter in deciding whether to extract the trees for timber production when the first signs of infection appear. Future research should concentrate on the anatomical properties and cell structure of wood in order to clearly observe the level of infection by *C. deuterocubensis* for better infection severity classification.

Author Contributions: Conceptualization, R.D., P.M.T. and S.S.; methodology, P.M.T., R.D., A.C.I., M.S.H. and P.S.K.; formal analysis, R.D. and S.H.L.; investigation, R.D., M.S.H. and P.S.K.; data curation, R.D., P.M.T., S.H.L. and P.S.K.; writing—original draft preparation, R.D., S.H.L., S.S. and P.A.; writing—review and editing, R.D., S.H.L., T.K. and P.A.; supervision, S.H.L., P.M.T. and S.S.; project administration, P.M.T.; funding acquisition, P.M.T., S.H.L., T.K. and S.S. All authors have read and agreed to the published version of the manuscript.

Funding: This research was funded by the Trans-disciplinary Research Grant Scheme (TRGS 2018-1), Reference code: TRGS/1/2018/UPM/01/2/3 (vote number: 5535800) by Ministry of Higher Education (MOHE), Malaysia.

Institutional Review Board Statement: Not applicable.

Informed Consent Statement: Not applicable.

Data Availability Statement: Not applicable.

Acknowledgments: The authors would like to express their gratitude to Sabah Softwoods Berhad (SSB) staff and management for providing the wood materials, and to the Institute of Tropical Forestry and Forest Products and Faculty of Forestry and Environment, Universiti Putra Malaysia for the facilities and assistance provided.

Conflicts of Interest: The authors declare no conflict of interest.

References

- Luo, J.; Arnold, R.; Ren, S.; Jiang, Y.; Lu, W.; Peng, Y.; Xie, Y. Veneer grades, recoveries, and values from 5-year-old eucalypt clones. *Ann. For. Sci.* **2013**, *70*, 417–428. [\[CrossRef\]](#)
- Ahmad, M.F.; Hishamuddin, M.S. Trees Diseases and Disorders in Urban Forests of Peninsular Malaysia. In *Urban Forestry and Arboriculture in Malaysia “An Interdisciplinary Research Perspective”*; Maruthaveeran, S., Chen, W.Y., Morgenroth, J., Eds.; Springer: Berlin/Heidelberg, Germany, 2022; Volume 1, pp. 83–104.
- Alves, I.C.N.; Gomide, J.L.; Colodette, J.L.; Silva, H.D. Technological characterization of *Eucalyptus benthamii* wood for kraftpulp production. *Cienc. Florestal.* **2011**, *21*, 167–174. [\[CrossRef\]](#)
- Bassa, A.G.M.C.; Francides, G.D.S.J.; Sacon, V.M. Mixtures of *Eucalyptus grandis* x *Eucalyptus urophylla* and *Pinus taeda* woodchips for kraft pulp production by Lo-Solids process. *Scientia Forestalis.* **2007**, *75*, 19–30.
- Nakabonge, G.; Roux, J.; Gryzenhout, M.; Wingfield, M.J. Distribution of *Chrysoporthe* canker pathogens on *Eucalyptus* and *Syzygium* spp. in eastern and southern Africa. *Plant Dis.* **2006**, *90*, 734–740. [\[CrossRef\]](#)
- Leonardi, G.D.A.; Carlos, N.A.; Mazzafera, P.; Balbuena, T.S. *Eucalyptus urograndis* stem proteome is responsive to short-term cold stress. *Genet. Mol. Biol.* **2015**, *38*, 191–198. [\[CrossRef\]](#)
- Lee, S.H.; Lum, W.C.; Antov, P.; Kristak, L.; Paridah, M.T. Engineering Wood Products from *Eucalyptus* spp. *Adv. Mater. Sci. Eng.* **2022**, *2022*, 8000780.
- Carvalho, A.M. The valuation of *Eucalyptus grandis* x *Eucalyptus urophylla* hybrid wood through the production of small dimension sawn wood, pulpwood and fuelwood. *Sci. Forestalis.* **2000**, *59*, 61–76.
- Jiang, X.M.; Ye, K.L.; Lu, J.X.; Zhao, Y.K.; Yin, Y.F. *Guide on Utilisation of Eucalyptus and Acacia Plantations in China for Solid Wood Products. The Final Technical Report for: Improved and Diversified Use of Tropical Plantation Timbers in China to Supplement Diminishing Supplies from Natural Forests “ITTO Project PD69/01 REV.2”*; Science Press: Beijing, China, 2007; p. 181.
- Labate, C.A.; de Assis, T.F.; Oda, S.; Mello, E.J.; Mori, E.S.; de Moraes, M.L.T.; Barreto, L.P.; Gonzalez, E.R.; Alfenas, A.C.; Edival, A.; et al. *Eucalyptus*. In *Compendium of Transgenic Crop Plants: Transgenic Forest Tree Species*; Cole, C., Hall, T.C., Eds.; Wiley: New York, NY, USA, 2008; Volume 9, pp. 35–99. ISBN 978-1-405-16924-0.
- Brigatti, R.A.; Ferreira, M.; Silva, A.P.; Freitas, M. Comparative study of the behavior of some *Eucalyptus* spp. hybrids. *Silvicultura* **1983**, *32*, 761–764.
- Ikemori, Y.K.; Campinhos, E. *Eucalyptus urophylla* x *Eucalyptus grandis* seed production by open pollination—Preliminaries results. *Silvicultura* **1983**, *8*, 306–308.
- Bertolucci, F.; Rezende, G.; Penchel, R. Production and use of eucalyptus hybrids. *Silvicultura* **1995**, *51*, 12–16.
- Sembiring, N.; Napitupulu, H.L.; Sembiring, M.T.; Ishak, A.; Gunawan, H.A. Fulfilling Eucalyptus raw materials for pulp and paper production plants. In *IOP Conference Series: Earth and Environmental Science*; IOP Publishing: Bristol, UK, 2021; Volume 912, p. 012008. [\[CrossRef\]](#)
- Scanavaca, L., Jr.; Garcia, J.N. Yield in sawed wood of *Eucalyptus urophylla*. *Sci. For.* **2003**, *63*, 32–43.
- Ahmad, Z.Y. Planting of Eucalyptus in Malaysia. *Acta Sci. Agric.* **2020**, *4*, 139–140.
- Ahmad, Z.Y.; Hassan, N.H.; Loon, N.T.; Heng, L.H.; Zorkarnain, F.A. Comparing the early growth performance of plantation-grown Eucalyptus hybrid and *Eucalyptus pellita*, South Johore, Peninsular Malaysia. *WJARR* **2020**, *6*, 234–238.
- Muhammad, S.A.R. Isolation and Identification of Causal Disease of *Eucalyptus pellita*. Bachelor’s Thesis, Universiti of Malaysia, Sarawak, Kota Samarahan, Malaysia, 2012.
- Suzuki, H.; Marincowitz, S.; Wingfield, B.D.; Wingfield, M.J. Genetic diversity and population structure of *Chrysoporthe deuterocubensis* isolates from Melastoma and Eucalyptus in Malaysia and Indonesia. *For. Pathol.* **2022**, *52*, 12762. [\[CrossRef\]](#)
- Rauf, M.R.B.A.; McTaggart, A.R.; Marincowitz, S.; Barnes, I.; Japarudin, Y.; Wingfield, M.J. Pathogenicity of *Chrysoporthe deuterocubensis* and *Myrtoporthe bodenii* gen. et sp. nov. on Eucalyptus in Sabah, Malaysia. *Australas. Plant Pathol.* **2019**, *49*, 53–64. [\[CrossRef\]](#)
- Gezahgne, A. Main Diseases of Eucalyptus Species in Ethiopia. In *Eucalyptus Species Management, History, Status and Trends in Ethiopia*; Wubalem, G., Lopez, T., Eds.; Technical University of Madrid: Madrid, Spain, 2010; pp. 351–369.
- Lee, S.S. Observations on the successes and failures of acacia plantations in Sabah and Sarawak and the way forward. *J. Trop. For. Sci.* **2018**, *30*, 468–475. [\[CrossRef\]](#)
- Forestry Economics and Policy Division. *Global Review of Forest Pests and Diseases*; Food and Agriculture Organization (FAO): Rome, Italy, 2009; p. 235. ISBN 978-92-5-106208-1.
- Dahali, R.; Md Tahir, P.; Roseley, A.S.M.; Hua, L.S.; Bakar, E.S.; Ashaari, Z.; Abdul Rauf, M.R.; Zainuddin, N.A.; Mansoor, N.S. Influence of *Chrysoporthe deuterocubensis* Canker Disease on the Physical and Mechanical Properties of *Eucalyptus urograndis*. *Forests* **2021**, *12*, 639. [\[CrossRef\]](#)

25. Dahali, R.; Lee, S.H.; Md Tahir, P.; Bakar, E.S.; Muhammad Roseley, A.S.; Ibrahim, S.A.; Mohd Yusof, N.; Mohammad Suffian James, R. Tahir, P.; Bakar, E.S.; Muhammad Roseley, A.S.; Ibrahim, S.A.; Mohd Yusof, N.; Mohammad Suffian James, R. Influence of *Chrysosporthe deuterocubensis* Canker Disease on the Machining Properties of *Eucalyptus urograndis*. *Forests* **2022**, *13*, 1366. [[CrossRef](#)]
26. Alvares, C.A.; Stape, J.L.; Sentelhas, P.C.; Goncalves, J.L.D.M.; Sparovek, G. Koppen's climate classification map for Brazil. *Meteorol. Z.* **2014**, *22*, 711–728. [[CrossRef](#)]
27. TAPPI Standard, T 257 cm-02; Sampling and Preparing Wood for Chemical Analysis. TAPPI: Atlanta, GA, USA, 2002.
28. Nandiyanto, A.B.D.; Oktiani, R.; Ragadhita, R. How to Read and Interpret FTIR Spectroscopy of Organic Material. *Indones. J. Sci. Technol.* **2019**, *4*, 97–118. [[CrossRef](#)]
29. ASTM Standard D2017; Standard Test Method of Accelerated Laboratory Test of Natural Decay Resistance of Woods. ASTM International: West Conshohocken, PA, USA, 2012.
30. Bakar, E.S.; Hao, J.; Ashaari, Z. Durability of phenolic-resin-treated oil palm wood against subterranean termites a white-rot fungus. *Int. Biodeterior. Biodegrad.* **2013**, *85*, 126–130. [[CrossRef](#)]
31. AWWA Standard E1-09; Standard Method for Laboratory Evaluation to Determine Resistance to Subterranean Termites. American Wood Protection Association: Birmingham, AL, USA, 2012.
32. Arinana, A.; Philippines, I.; Koesmaryono, Y.; Sulaeha, S.; Maharani, Y.; Indarwatmi, M. The daytime indoor and outdoor temperatures of the subterranean termite *Coptotermes curvignathus* Holmgren (*Isoptera: Rhinotermitidae*) tunnel. In *IOP Conference Series: Earth and Environmental Science*; IOP Publishing: Bristol, UK, 2021; Volume 807, p. 022027. [[CrossRef](#)]
33. Kuswanto, E.; Ahmad, I.; Dungani, R. Threat of subterranean termites attack in the Asian countries and their control: A review. *Asian J. Appl. Sci.* **2015**, *8*, 227–239. [[CrossRef](#)]
34. Dahali, R.; Hua, L.S.; Ashaari, Z.; Bakar, E.S.; Ariffin, H.; San, K.P.; Bawon, P.; Salleh, Q.N. Durability of superheated steam-treated light red meranti (*Shorea* spp.) and kedondong (*Canarium* spp.) wood against white rot fungus and subterranean termite. *Sustainability* **2020**, *12*, 4431. [[CrossRef](#)]
35. Anantharaju, T.; Kaur, G.; Gajalakshmi, S.; Abbasi, S.A. Sampling and identification of termites in Northeastern. *Puducherry J. Entomol. Zool. Stud.* **2014**, *2*, 225–230.
36. Rilatupa, J. 2006 Kondisi komponen konstruksi bangunan tinggi dan hubungannya dengan karakteristik serangan rayap. *J. Sains Teknol. EMAS* **2006**, *16*, 71–86.
37. SNI Standard 01.7207; Standard Method for Test of Resistance Wood and Wood Products against Wood Destroying Organisms “Ujian ketahanan kayu dan produk kayu terhadap organisme perusak kayu”. Indonesian National Standard (Standar Nasional Indonesia): Jakarta, Indonesia, 2006.
38. Terzi, E.; Kartal, S.N.; Muin, M.; Hassanin, A.H.; Hamouda, T.; Kulic, A.; Candan, Z. Biological Performance of Novel Hybrid Green Composites Produced from Glass Fibers and Jute Fabric Skin by the VARTM Process. *BioResources* **2018**, *13*, 662–677. [[CrossRef](#)]
39. Reddy, N.; Yang, Y. Biofibers from agricultural byproducts for industrial applications. *Trends Biotechnol.* **2005**, *23*, 22–27. [[CrossRef](#)]
40. Ferrari, R.; Gautier, V.; Silar, P. Lignin degradation by ascomycetes Wood Degradation and Ligninolytic Fungi. *Adv. Bot. Res.* **2021**, *9*, 77–113.
41. Savory, J.G.; Pinion, L.C. Chemical aspects of decay of beech wood by *Chaetomium globosum*. *Int. J. Biol. Chem. Phys. Technol. Wood* **1958**, *12*, 99–103.
42. Andlar, M.; Rezić, T.; Mardetko, N.; Kracher, D.; Ludwig, R.; Santek, B. Lignocellulose degradation: An overview of fungi and fungal enzymes involved in lignocellulose degradation. *Eng. Life Sci.* **2018**, *18*, 768–778. [[CrossRef](#)]
43. Janusz, G.; Pawlik, A.; Sulej, J.; Swiderska-Burek, U.; Jarosz-Wilkolazka, J.; Paszczyoski, A. Lignin degradation: Microorganisms, enzymes involved, genomes analysis and evolution. *FEMS Microbiol. Rev.* **2017**, *41*, 941–962. [[CrossRef](#)]
44. Kirk, T.K.; Farrell, R.L. Enzymatic “combustion”: The microbial degradation of lignin. *Annu. Rev. Microbiol.* **1987**, *41*, 465–505. [[CrossRef](#)]
45. Mafia, R.G.; Ferreira, M.A.; Zauza, E.A.V.; Silva, J.F.; Colodette, J.L.; Alfenas, A.C. Impact of *Ceratocystis* wilt on Eucalyptus tree growth and cellulose pulp yield. *For. Pathol.* **2013**, *43*, 379–385. [[CrossRef](#)]
46. Foelkel, C.E.B.; Zvinakevicius, C.; Andrade, J.M. A qualidade do eucalipto. *Silvicultura* **1978**, *2*, 53–62.
47. Pereira, B.L.; Carneiro, A.C.; Carvalho, A.M.; Colodette, J.L.; Oliveira, A.C.; Fontes, M.P. Influence of Chemical Composition of Eucalyptus Wood on Gravimetric Yield and Charcoal Properties. *Bioresources* **2013**, *8*, 4574–4592. [[CrossRef](#)]
48. Rowell, R.M.; Pettersen, R.; Han, J.S.; Rowell, J.S.; Tshabalala, M.A. *Cell wall chemistry*, In *Handbook of Wood Chemistry and Wood Composites*; Rowell, R.M., Ed.; CRC Press: Boca Raton, FL, USA, 2005.
49. Shebani, A.N.; Van Reenen, A.J.; Meincken, M. The effect of wood extractives on the thermal stability of different wood species. *Thermochim. Acta* **2008**, *471*, 43–50. [[CrossRef](#)]
50. Fengel, D.; Wegener, G. *Wood, Chemistry, Ultrastructure, Reactions*; Walter de Gruyter: New York, NY, USA, 1984.
51. Stenius, P. *Paper Making Science and Technology: Forest Products Chemistry (Book 3)*; Fapet: Helsinki, Finland, 2000.
52. Gunduz, G.; Oral, M.A.; Akyuz, M.; Aydemir, D.; Yaman, B.; Asik, N.; Bulbul, A.S.; Allahverdiyev, S. Physical, morphological properties and raman spectroscopy of chestnut blight diseased *Castanea sativa* Mill. wood. *CERNE* **2016**, *22*, 43–58. [[CrossRef](#)]
53. Fernandes, B.V.; Zanoncio, A.J.V.; Furtado, E.L.; Andrade, H.B. Damage and Loss Due to *Ceratocystis fimbriata* in Eucalyptus Wood for Charcoal Production, “Eucalyptus fungal loss”. *BioResources* **2014**, *9*, 5473–5479. [[CrossRef](#)]

54. Mafia, R.G.; Santos, P.C.; Demuner, B.J.; Massoquete, A.; Sarto rio, R.C. Eucalyptus wood decay: Effects on productivity and quality of cellulose. *For. Pathol.* **2012**, *42*, 321–329. [[CrossRef](#)]
55. Souza, S.E.; Sansigolo, C.A.; Furtado, E.L.; de Jesus, W.C.; Oliveira, R.R. Influencia do cancro basal em *Eucalyptus grandis* nas propriedades da madeira e polpacao Kraft. *Sci. Florest.* **2010**, *38*, 447–457.
56. Leśniewska, J.; Öhman, D.; Krzesłowska, M.; Kushwah, S.; Barciszewska-Pacak, M.; Kleczkowski, L.A.; Sundberg, B.; Moritz, T.; Mellerowicz, E.J. Defense responses in aspen with altered pectin methylesterase activity reveal the hormonal inducers of tyloses. *Plant Physiol.* **2017**, *173*, 1409–1419. [[CrossRef](#)] [[PubMed](#)]
57. Nicholson, R.L.; Hammerschmid, T.R. Phenolic compounds and their role in disease resistance. *Ann. Rev. Phytopathol.* **1992**, *30*, 369–389. [[CrossRef](#)]
58. Vance, C.P.; Kirk, T.K.; Sherwood, R.T. Lignification as a mechanism of disease resistance. *Ann. Rev. Phytopathol.* **1980**, *18*, 259–288. [[CrossRef](#)]
59. Kuc, J. Concepts and direction of induced systemic resistance in plants and its application. *Eur. J. Plant Pathol.* **2001**, *107*, 7–12. [[CrossRef](#)]
60. Shigo, A.I.; Marx, H.G. 1977: Compartmentalization of decay in trees. *USDA Agric. Inform. Bull.* **1977**, *405*, 1–73.
61. Elgersma, D.M. Tylose formation in elms after inoculation with *Ceratocystis ulmi*, a possible resistance mechanism. *Eur. J. Forest Pathol.* **1973**, *79*, 218–220. [[CrossRef](#)]
62. El Modafar, C.; Clerivet, A.; Macheix, J.J. Flavan accumulation in stems of *Platanus acerifolia* seedlings inoculated with *Ceratocystis fimbriata* f. sp. platani, the canker stain disease agent. *Can. J. Bot.* **1996**, *74*, 1982–1987. [[CrossRef](#)]
63. Broda, M.; Popescu, C.M.; Curling, S.F.; Timpu, D.I.; Ormondroyd, G.A. Effects of Biological and Chemical Degradation on the Properties of Scots Pine Wood-Part I: Chemical Composition and Microstructure of the Cell Wall. *Materials* **2022**, *15*, 2348. [[CrossRef](#)]
64. Hua, L.S.; Ashaari, Z.; Ang, A.F.; Halip, J.A.; Lum, W.C.; Dahali, R.; Halis, R. Effects of two-step post heat-treatment in palm oil on the properties of oil palm trunk particleboard. *Ind. Crop. Prod.* **2018**, *116*, 249–258.
65. Esteves, B.; Videira, R.; Pereira, H. Chemistry and ecotoxicity of heat-treated pine wood extractives. *Wood Sci Technol.* **2011**, *45*, 661–676. [[CrossRef](#)]
66. Coates, J. Interpretation of infrared spectra, a practical approach. *Encycl. Anal. Chem.* **2000**, *12*, 10815–10837.
67. Esteves, B.; Marques, A.V.; Domingos, I.; Pereira, H. Chemical changes of heat-treated pine and eucalypt wood monitored by FTIR. *Maderas. Cienc. Y Tecnol.* **2013**, *15*, 245–258. [[CrossRef](#)]
68. Moharram, M.; Mahmoud, O. FTIR Spectroscopic Study of the Effect of Microwave Heating on the Transformation of Cellulose I into Cellulose II during Mercerization. *J. Appl. Pol. Sci.* **2008**, *107*, 30–36. [[CrossRef](#)]
69. Spiridon, I.; Teaca, C.; Bodirlau, R. Structural changes evidenced by FTIR spectroscopy in cellulosic materials after pre-treatment with ionic liquid and enzymatic hydrolysis. *Bioresources* **2011**, *6*, 400–413. [[CrossRef](#)]
70. Li, J.; Li, B.; Zhang, X. Comparative studies of heat degradation between larch lignin and Manchurian ash lignin. *Polym. Degrad. Stab.* **2002**, *78*, 279–285. [[CrossRef](#)]
71. Kotilainen, R.; Toivannen, T.; Alen, R. FTIR monitoring of chemical changes in softwood during heating. *J. Wood Chem. Technol.* **2002**, *20*, 307–320. [[CrossRef](#)]
72. Huang, Y.; Wang, L.; Chao, Y.; Nawawi, D.S.; Akiyama, T.; Yokoyama, T.; Matsumoto, Y. Analysis of lignin aromatic structure in wood based on the IR spectrum. *J. Wood Chem. Technol.* **2012**, *32*, 294–303. [[CrossRef](#)]
73. Gelbrich, J.; Mai, C.; Miltz, H. Chemical changes in wood degraded by bacteria. *Int. Biodeterior. Biodegrad.* **2008**, *61*, 24–32. [[CrossRef](#)]
74. Pena, M.M.G.; Curling, S.F.; Hale, M.D.C. On the effect of heat on the chemical composition and dimensions of thermally-modified wood. *Polym. Degrad. Stab.* **2009**, *94*, 2184–2193. [[CrossRef](#)]
75. Riley, R.; Salamov, A.A.; Brown, D.W.; Nagy, L.G.; Floudas, D.; Held, B.W.; Levasseur, A.; Lombard, V.; Morin, E.; Otilar, R.; et al. Extensive sampling of basidiomycete genomes demonstrates inadequacy of the white-rot/brown-rot paradigm for wood decay fungi. *Proc. Natl. Acad. Sci. USA* **2014**, *111*, 9923–9928. [[CrossRef](#)]
76. Schilling, J.S.; Kaffenberger, J.T.; Held, B.W.; Ortiz, R.; Blanchette, R.A. Using wood rot phenotypes to illuminate the “gray” among decomposer fungi. *Front. Microbiol.* **2020**, *11*, 1288. [[CrossRef](#)] [[PubMed](#)]
77. Rouhier, M.M. Wood as a hostile habitat for ligninolytic fungi “Wood Degradation and Ligninolytic Fungi”. *Adv. Bot. Res.* **2021**, *99*, 115–149.
78. Clerivet, A.; El Modafar, C. Vascular modifications in *Platanus acerifolia* seedlings inoculated with *Ceratocystis fimbriata* f. sp. platani. *Eur. J. Forest Pathol.* **1994**, *24*, 1–10. [[CrossRef](#)]
79. Rioux, D.; Nicole, M.; Simard, M.; Ouellette, G.B. Immunocytochemical evidence that secretion of pectin occurs during gel (gum) and tylosis formation in trees. *Phytopathology* **1998**, *88*, 494–505. [[CrossRef](#)] [[PubMed](#)]
80. Clerivet, A.; Deon, V.; Alami, I.; Lopez, F.; Geiger, J.P.; Nicole, M. Tyloses and gels associated with cellulose accumulation in vessels are responses of plane tree seedlings (*Platanus acerifolia*) to the vascular fungus *Ceratocystis fimbriata* f. sp. platani. *Trees* **2000**, *15*, 25–31. [[CrossRef](#)]
81. Malaysian Timber Industrial Board (MTIB). Medium Hardwood Eucalyptus. In *100 Malaysian Timbers*, 2010th ed.; Malaysian Timber Industry Board: Kuala Lumpur, Malaysia, 2010; pp. 132–133.
82. Eucalyptus Urophylla. Available online: https://en.wikipedia.org/wiki/Eucalyptus_urophylla (accessed on 20 December 2022).

83. Eucalyptus grandis. Available online: https://en.wikipedia.org/wiki/Eucalyptus_grandis (accessed on 20 December 2022).
84. Bayle, G.K. Ecological and social impacts of Eucalyptus tree plantation on the environment. *Biodivers. Conserv. Bioresour. Manag.* **2019**, *5*, 93–104. [[CrossRef](#)]
85. Food and Agriculture Organization (FAO). *Flavours and Fragrances of Plant Origin*; Food and Agriculture Organization: Rome, Italy, 1995.
86. Toloza, A.C.; Lucia, A.; Zerba, Z.; Masuh, H.; Picollo, M.I. Interspecific hybridization of Eucalyptus as a potential tool to improve the bioactivity of essential oils against permethrin-resistant head lice from Argentina. *Bioresour. Technol.* **2008**, *99*, 7341–7347. [[CrossRef](#)]
87. Guenther, E. *The Essential Oils*; Krieger Publishing Company: Malabar, FL, USA, 1972.

Disclaimer/Publisher’s Note: The statements, opinions and data contained in all publications are solely those of the individual author(s) and contributor(s) and not of MDPI and/or the editor(s). MDPI and/or the editor(s) disclaim responsibility for any injury to people or property resulting from any ideas, methods, instructions or products referred to in the content.